AcrB drug-binding pocket substitution confers clinically relevant resistance and altered substrate specificity

Jessica M. A. Blair[a], Vassiliy N. Bavro[a], Vito Ricci[a], Niraj Modi[b], Pierpaolo Cacciotto[c], Ulrich Kleinekathöfer[b], Paolo Ruggerone[c], Attilio V. Vargiu[c], Alison J. Baylay[a], Helen E. Smith[a], Yvonne Brandon[a], David Galloway[a], and Laura J. V. Piddock[a,1]

[a]Antimicrobials Research Group, School of Immunity and Infection, College of Medical and Dental Sciences, Institute of Microbiology and Infection, The University of Birmingham, Birmingham B15 2TT, United Kingdom; [b]School of Engineering and Science, Jacobs University Bremen, 28759 Bremen, Germany; and [c]Department of Physics, University of Cagliari, 09042 Monserrato, Italy

Edited by Hiroshi Nikaido, University of California, Berkeley, CA, and approved February 13, 2015 (received for review October 24, 2014)

The incidence of multidrug-resistant bacterial infections is increasing globally and the need to understand the underlying mechanisms is paramount to discover new therapeutics. The efflux pumps of Gram-negative bacteria have a broad substrate range and transport antibiotics out of the bacterium, conferring intrinsic multidrug resistance (MDR). The genomes of pre- and posttherapy MDR clinical isolates of *Salmonella* Typhimurium from a patient that failed antibacterial therapy and died were sequenced. In the posttherapy isolate we identified a novel G288D substitution in AcrB, the resistance-nodulation division transporter in the AcrAB-TolC tripartite MDR efflux pump system. Computational structural analysis suggested that G288D in AcrB heavily affects the structure, dynamics, and hydration properties of the distal binding pocket altering specificity for antibacterial drugs. Consistent with this hypothesis, recreation of the mutation in standard *Escherichia coli* and *Salmonella* strains showed that G288D AcrB altered substrate specificity, conferring decreased susceptibility to the fluoroquinolone antibiotic ciprofloxacin by increased efflux. At the same time, the substitution increased susceptibility to other drugs by decreased efflux. Information about drug transport is vital for the discovery of new antibacterials; the finding that one amino acid change can cause resistance to some drugs, while conferring increased susceptibility to others, could provide a basis for new drug development and treatment strategies.

efflux | antimicrobial resistance | AcrB | whole genome sequencing

The incidence of multidrug-resistant (MDR, also used herein for "multidrug resistance") bacterial infections is increasing, and the 2013 World Economic Forum Global Risks report listed antibiotic-resistant bacteria as one of the greatest threats to human health (1). Resistance-nodulation division (RND) efflux pumps of Gram-negative bacteria confer intrinsic and acquired MDR in clinically relevant infections by exporting antibiotics out of the bacterial cell, allowing bacteria to survive at increased drug concentrations.

To date the best-characterized efflux pump is AcrAB-TolC of *Escherichia coli*, composed of the inner membrane RND antiporter AcrB that functions in a tripartite assembly with a periplasmic adaptor protein, AcrA, and the outer membrane channel, TolC. The AcrB pump is an asymmetric homotrimer whose monomers undergo a functional rotation through three states: access, binding, and extrusion (labeled A, B, and E, respectively) to pump substrates from the periplasm, or outer leaflet of the inner membrane, to outside of the cell (2, 3). Drug binding within AcrB is complex. The distal binding pocket has a phenylalanine-rich region that binds low-molecular-weight drugs and a proximal binding pocket and vestibule bind larger compounds such as erythromycin (4, 5).

To date, MDR in clinically relevant infections mediated by RND efflux pumps, including AcrB, has been documented to be due to overexpression of the efflux pump and concomitant increased efflux of antibiotics from the bacterial cell (6). Overproduction of efflux pumps can occur via four mechanisms: (*i*) mutation of the local repressor gene (7, 8), (*ii*) mutation in a global regulatory gene (9, 10), (*iii*) mutation of the promoter region of the efflux pump gene (11), or (*iv*) insertion elements upstream of the transporter gene (12, 13).

This study focused on elucidating the mechanism of resistance in a unique set of clinical isolates collected over the course of a complex *Salmonella* infection (Fig. S1) (14, 15). The isolates were obtained from a 52-y-old male patient admitted for repair of a leaking abdominal aortic aneurysm graft. *Salmonella* Typhimurium (L3) was isolated before ciprofloxacin treatment and was susceptible to ampicillin, sulphonamide, trimethoprim, cefuroxime, chloramphenicol, gentamicin, and ciprofloxacin. Over the course of the infection the patient received i.v. ciprofloxacin, oral ciprofloxacin, i.v. ceftazidime, and i.v. aztreonam. Isolates were taken throughout infection, and during treatment MDR strains were isolated. L18, the last MDR strain to be isolated, was from wound drainage fluid when the patient had received no antibiotics for 2 wks. The patient died soon afterward with the infection unresolved. Compared with the pretherapy isolate L3, the MDR posttherapy isolate, L18, was less susceptible to numerous agents, including ciprofloxacin and β-lactams, and accumulated less ciprofloxacin and Hoechst dye (16). This set of isolates has provided a unique opportunity to investigate in vivo evolution of MDR in response to clinically validated courses of antimicrobial treatment.

Here, we report that whole genome sequencing revealed a new mechanism of clinically significant MDR selected during therapy:

Significance

Genome sequencing of a multidrug-resistant clinical isolate of *Salmonella* Typhimurium from a patient that failed ciprofloxacin therapy revealed a mutation in the efflux pump gene, *acrB*. Computational modelling revealed that the G288D substitution changed the binding of drugs to the distal binding pocket of AcrB. The mutation was recreated in an unrelated *Salmonella* strain and also in *Escherichia coli*; in both species the efflux of ciprofloxacin was increased by the mutation, explaining its resistant phenotype. This is the first time a substitution within an efflux pump protein has been shown to cause drug resistance. Importantly, the finding that one amino acid change can cause resistance to some drugs, but susceptibility to others, informs those developing new antibiotics.

Author contributions: J.M.A.B., V.N.B., P.C., U.K., P.R., A.V.V., and L.J.V.P. designed research; J.M.A.B., V.N.B., V.R., N.M., P.C., U.K., P.R., A.V.V., A.J.B., H.E.S., Y.B., and D.G. performed research; J.M.A.B., V.N.B., N.M., P.C., U.K., P.R., and A.V.V. analyzed data; and J.M.A.B., V.N.B., P.C., U.K., P.R., A.V.V., and L.J.V.P. wrote the paper.

The authors declare no conflict of interest.

This article is a PNAS Direct Submission.

[1]To whom correspondence should be addressed. Email: l.j.v.piddock@bham.ac.uk.

This article contains supporting information online at www.pnas.org/lookup/suppl/doi:10.1073/pnas.1419939112/-/DCSupplemental.

Table 1. Antimicrobial susceptibility of isolates and substitution in AcrB

Strain	Weeks posttherapy	MIC, μg/mL Cip	Nal	Chl	Tet	Atm	Caz	AcrB residue 288
L3	0	0.015	2	2	1	0.06	0.12	G
L10	1	**0.06**	**8**	**8**	2	0.12	0.5	G
L11*	3	**0.03**	**16**	**8**	2	**0.25**	0.25	G
L12	3	**0.5**	**64**	**32**	**8**	**0.5**	1	D
L13*	3	**0.5**	**64**	**16**	**8**	**0.5**	0.5	D
L6	5	**0.5**	**64**	**32**	**8**	**0.5**	0.5	D
L16	17	**0.5**	**64**	**32**	**8**	**0.5**	1	D
L18†	19	**0.5**	**64**	**32**	**8**	**0.5**	2	D

Experiments were performed on at least three separate occasions. MIC data presented are the mode values. MIC values shown in bold are two or more dilutions higher than for the pretherapy isolate, L3. Isolates in bold are those with G288D substitution. Atm, aztreonam; Caz, ceftazidime; Chl, chloramphenicol; Cip, ciprofloxacin; Nal, nalidixic acid; Tet, tetracycline.
*Mutation in *gyrA* (19).
†Rare mutation at residue 464 in *gyrB* (17).

substitution in a transporter protein, which altered the specificity of the efflux pump for antibacterial drugs. The structural impact of the substitution was investigated by molecular dynamics (MD) simulations.

Results

The Genomes of Pre- and Posttherapy Isolates Differ by Five SNPs. To identify mutations associated with the emergence of MDR, *Salmonella enterica* serovar Typhimurium L3 (pretherapy) and L18 (5 mo posttherapy) were sequenced by Illumina sequencing and compared with the published genome sequence of *Salmonella enterica* serovar Typhimurium LT2. Five SNPs relative to LT2 were identified in L18 that were not present in L3, suggesting that they arose during the time course of the infection (Table S1). Targeted PCR and Sanger sequencing of specific genes confirmed all mutations. One SNP occurred in an intergenic region, and the remaining four caused changes in the protein sequence of affected genes (nonsynonymous SNPs). These included a mutation at residue 464 of *gyrB,* which encodes a mutant B subunit of the topoisomerase II enzyme; the effect of this mutation has been previously studied in detail and confers quinolone resistance but not MDR (17). The genome sequencing also revealed a novel substitution from a glycine to an aspartic acid at residue 288 of AcrB.

The Appearance of the AcrB Substitution Coincides with MDR. Antibiotic resistance, particularly to ciprofloxacin [minimum inhibitory concentration (MIC) ≥0.5 μg/mL], occurred and increased in the isolates along the time course of infection (Table 1; susceptibility data for other antibiotics have been previously published and are shown in Table S2) (14, 15, 18). Previously, the MDR was attributed to increased expression of the *acrB* transcript (18). Indeed, measurement of *acrB* expression using an *acrAB* promoter–GFP fusion confirmed increased *acrB* expression in all strains isolated after the onset of therapy but the expression level did not correlate with the MDR phenotype. For example, *acrB* expression in L10 was not significantly different from that of L18, but L18 was more resistant. However, the level of MDR did correlate with which residue was present at position 288 of AcrB; the isolates with the highest level of MDR all carried the G288D substitution in AcrB. Isolates with an aspartic acid at residue 288 were two- to fourfold less susceptible to antibiotics compared with those with glycine at the same residue (Table 1). The changes in susceptibility were sufficient to confer clinically relevant resistance to the drugs used to treat the patient.

The AcrB G288D Substitution Causes Ciprofloxacin Resistance. To confirm the importance of AcrB to the phenotype, *acrB* was inactivated in the MDR isolate, L18, to give strain L1299 and susceptibility to known substrates of AcrB was determined. Decreased MICs of ciprofloxacin, nalidixic acid, chloramphenicol, and tetracycline, to within one dilution of those for the pretherapy isolate L3, were obtained (Table 2).

To further investigate the effect of the G288D substitution, the wild-type and mutant *acrB* sequences were cloned into pWKS30 and transformed into the multidrug-susceptible L1299 (L18 with *acrB* deleted; Table S3). Similar levels of wild-type (L1351) and mutant (L1315) *acrB*/AcrB were expressed (as shown by RT-PCR and Western blotting; Table S4 and Fig. S2). Apart from ciprofloxacin, where only a modest decrease in susceptibility was seen (due to the mutation in *gyrB*) (19), L18 Δ*acrB* with wild-type AcrB (L1351) had susceptibility to antibiotics similar to the pretherapy isolate L3. However, L18 Δ*acrB* with mutant G288D AcrB (L1315) was MDR and the MIC values were within one dilution of those for L18 for ciprofloxacin, nalidixic acid, chloramphenicol, and tetracycline. Interestingly, L1315 was more susceptible to minocycline and doxorubicin than L1351, which had wild-type AcrB. This was not seen in L18. This may be due to the level of AcrB being greater in L18 or due to one of the SNPs in another gene confounding the effect of the G288D substitution.

Computational Structural Biology Suggests That Drug Specificity Is Altered by G288D. Drug binding within AcrB is complex (20, 21) and is proposed to include several possible sites before extrusion including a vestibule and proximal and distal binding pocket. It has been suggested that low-molecular-mass compounds could bind directly to the phenylalanine-rich distal binding pocket (5, 20, 22), bypassing the proximal binding pocket and vestibule, which is (23) implicated in the recognition of larger compounds such as erythromycin (4, 5).

Structural alignment of the *S.* Typhimurium AcrB with the corresponding *E. coli* sequence shows high conservation of the distal pocket residues, suggesting a conserved mechanism of drug binding, and justifying the use of the *E. coli* structure as a guide for rationalization of the effect of the G288D substitution in L18 AcrB (Fig. S3). Residue 288 is also highly conserved in AcrB of other Enterobacteriaceae, suggesting an important structural role.

In the available crystal structures of AcrB in its apo- (PDB ID code 2J8S) (24) and in doxorubicin- (PDB ID code 4DX7) and minocycline-bound forms (PDB ID code 4DX5) (22), G288 is located in the middle of a beta strand, with the neighboring side chains pointing away from the pocket, suggesting that the substituted side chain will protrude into the pocket cavity. Hence, this bulky and charged aspartate residue will have a drastic impact on structure and

Table 2. The effect of *acrB* inactivation and the G288D mutation on antimicrobial susceptibility

Strain	Genotype	MIC, μg/mL Cip	Nal	Chl	Tet	Dxr	Min
L3	Pretherapy isolate	0.008	2	1	0.5	16	1
L18	Posttherapy isolate	0.5	32	8	4	>256	4
L1299	L18 *acrB::aph*	*0.015*	*1*	*1*	*0.5*	*4*	0.5
L1351	L1299 + p*acrB*-WT	*0.06*	*4*	*1*	*1*	*16*	*1*
L1315	L1299 + pG288D*acrB*	**0.25**	**16**	**4**	**2**	**4**	**0.25**

Experiments were carried out on at least three separate occasions and the mode value is presented. MIC values indicated in italic are two or more dilutions lower than for L18. MIC values indicated in bold indicate a difference between the MIC for L18 in which *acrB* has been inactivated and replaced with mutant (G288D) AcrB or wild-type (WT) AcrB. Chl, chloramphenicol; Cip, ciprofloxacin; Dxr, doxorubicin; Min, minocycline; Nal, nalidixic acid; Tet, tetracycline.

dynamics of this primarily hydrophobic pocket, not only by changing the electrostatic profile and polar environment of the cavity but also by causing steric clashes with several key residues involved in the hydrophobic stacking interactions with the substrate (Fig. 1). This in turn could affect the affinity to various drugs such as doxorubicin and minocycline whose binding positions have been identified by co-crystallization experiments (22) (Fig. 1). Indeed, previous studies have shown that several drug recognition determinants are deeply perturbed by a single substitution in a key region of the transporter (25, 26). To analyze possible changes in the distal binding pocket as a result of the mutation we built homology models of wild-type and G288D variant of *S.* Typhimurium AcrB using the crystal structure of wild-type *E. coli* AcrB (PDB ID code 2J8S) as a template. Subsequently, MD simulations in explicit solvent were carried out to identify major differences in structure and dynamics of the distal binding pocket. A tested, reduced model of the *S.* Typhimurium AcrB containing only the periplasmic domains was used as in previous computational studies on *E. coli* AcrB (27–29).

Comparison of representative structures (i.e., the conformations with the lowest rmsd from the averages) of the wild-type and mutant proteins revealed that the introduction of the aspartate induces local structural changes in the distal binding pocket (rmsd 3.1 Å). In particular, residues F178 and Q176 assume alternative conformation to avoid steric clashes with the aspartate and F136 shows a large displacement (Fig. 2). As a result, the radius of gyration calculated for the residues lining the distal pocket increased by ∼1 Å in the G288D variant (from ∼10.5 Å in wild type to ∼11.5 Å, Fig. S4). The radius of gyration is indicative of the level of compaction in the pocket and the measured variation indicates an increased size. However, these changes have only limited effect on the secondary structure of the distal binding pocket (Fig. S5*A*).

In addition to these local structural changes, the introduction of the aspartate increases the polarity of the otherwise highly hydrophobic distal binding pocket (Fig. 1) and hence may affect its hydration. To test this, radial distribution function (RDF) profiles, which show the probability of finding water molecules at a certain distance from the G288/D288 residues, were calculated. As anticipated in the mutant protein the D288 residue was found to have a higher probability of being surrounded by water molecules during the course of the simulation (Fig. 2, solid lines). The sharp peak at around 2.5 Å from D288 is due to the presence of the first hydration shell. To the contrary, water molecules are on

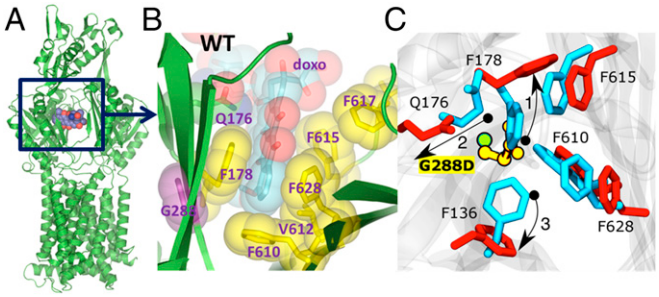

Fig. 1. Binding of doxorubicin to the AcrB monomer. (*A*) Overall view of the AcrB monomer bound to doxorubicin (shown in space fill) as per PDB ID code 4DX7 (22). (*B*) A close-up view of the doxorubicin binding pocket in the PDB ID code 4DX7, highlighting the principal residues involved in the drug binding. (*C*) Close view of the binding site where important residues are shown (blue, wild type; red, mutant). Owing to the presence of the side chain of the aspartate residue in the G288D mutant, the side chain of F178 tilts away in the G288D mutant compared with its orientation in the wild-type protein (denoted by the arrow and labeled as 1). In turn, the side chain orientation of the residue Q176 is also altered in the mutated protein (denoted by 2) with respect to the wild-type form. Finally, the side chain of F136 also changes orientation (denoted by 3).

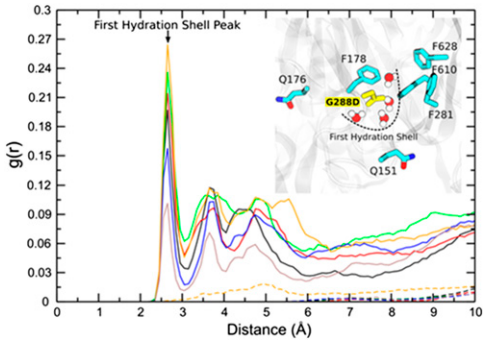

Fig. 2. RDF profiles indicating the distribution of water molecules near the D288 residue in the mutant (solid lines) protein and near the G288 residue in the wild-type protein (dashed lines). Differently colored lines (solid or dashed) represent the RDF profiles calculated from two different simulations and for each of the monomers of the AcrB protein. RDF profiles are calculated based on the distance between the water oxygen to center of mass of G288/D288 residue's side chain. (*Inset*) A representative snapshot of the presence of water molecules in the binding pocket of the G288D mutant protein. Water molecules at the corresponding positions are absent in the wild-type protein.

average absent in the close vicinity of G288, consistent with the more hydrophobic environment in the wild-type protein (Fig. 2, dashed lines). In addition, the mutant exhibits a notable change in residence time for water molecules within the distal pocket (Table S5).

We then analyzed the effect of the G288D substitution on doxorubicin, minocycline, and ciprofloxacin efflux. Doxorubicin and minocycline, although not clinically relevant, have been co-crystallized with *E. coli* AcrB, making phenotypic and structural data easier to correlate and interpret. We have compared these cocrystal structures with the results from the MD runs of the G288D variant. Consistent with MIC and drug accumulation data below, and based on the assumption that the binding of tetra-ring structures follows that in the cocrystal structures, the G288D substitution would result in pronounced steric clashes with both doxorubicin and minocycline, due also to displacement of amino acid F178 discussed above. Although an experimental structure of the ciprofloxacin–AcrB complex is lacking, a recent computational study (27) suggested that it binds to the bottom of the distal pocket, in a different position than doxorubicin (Fig. 3). In contrast to doxorubicin and minocycline, the G288D substitution should not impair the binding of ciprofloxacin; instead, the additional hydroxyl groups present in this compound may form hydrogen bonds with the introduced aspartate and resident waters, improving its recognition. In agreement with these hypotheses, G288D in L1315 (L18 Δ*acrB* pG288D*acrB)* not only led to increased susceptibility to doxorubicin and minocycline, likely due to decreased efflux, but also conferred increased efflux of, and decreased susceptibility to, ciprofloxacin and other fluoroquinolones (Table 2; MICs of more agents are shown in Table S6).

Although the differential effect of the mutation on the different classes of antibacterial drugs is not immediately obvious, it is notable that the efflux of more hydrophobic substrates such as doxorubicin and minocycline is correlated with the observed changes in the hydrophobicity of the distal binding pocket. Accordingly, minocycline and tetracycline seem differentially affected (Table 2), consistent with the former being 10-fold more lipophilic than the latter (Table S7).

***Salmonella* and *E. coli* Standard Reference Strains with the G288D AcrB Accumulate Less Ciprofloxacin and More Doxorubicin and Minocycline.** Given the above considerations about structure, dynamics, and hydration of G288D AcrB, along with our experimental MIC data, we predicted that the susceptibility to

MICROBIOLOGY

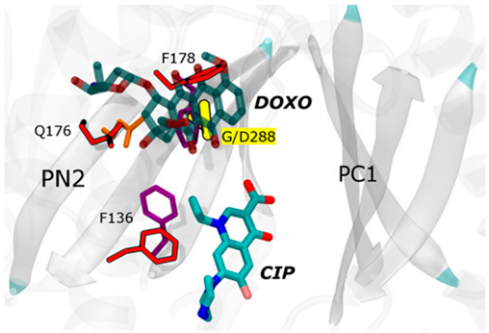

Fig. 3. Predicted effects of the mutation on the binding of the doxorubicin (DOXO) and ciprofloxacin (CIP) in the distal binding pocket. DOXO and CIP are rendered with transparent and solid thick sticks, respectively, colored by atom type. The Cα atom of G288 is rendered in green and the side chain of D288 with yellow sticks. Side chains of other most relevant residues are shown with thinner sticks, colored by residue type and red in wild type and G288D, respectively. The orientation of CIP is derived from the MD simulations (27), and that of DOXO is based on the experimental X-ray structure as from PDB ID code 4DX7 (22).

ciprofloxacin would be decreased in AcrB G288D strains owing to an increase in its efflux efficiency.

Both L3 and L18 have a mutation in *ramR* (16) and L18 has a mutation in *gyrB* (17); both of these are known to influence susceptibility to fluoroquinolones. Because SL1344 Δ*ramR* has MICs of doxorubicin and minocycline similar to those for L18 for these agents we hypothesize that the impact of the mutation in *ramR* in L18 masked the impact of the G288D substitution for these drugs. Therefore, to further investigate the effect of G288D, the mutant AcrB protein was expressed in two well-recognized standard antibiotic-susceptible reference strains, *S.* Typhimurium SL1344 and *E. coli* MG1655. In this way, unlike in L18, there were no other mutations that could affect antibacterial drug susceptibility and drug efflux. This allowed study of the G288D substitution in the absence of other mutations that could confound the phenotype. To explore whether efflux activity was altered due to the AcrB G288D substitution alone, the accumulation of ciprofloxacin, doxorubicin, and minocycline was measured. In both *Salmonella* and *E. coli* the strain expressing mutant AcrB (L1352 and I972, respectively) accumulated less ciprofloxacin than the strain expressing wild-type AcrB (L1365 and I971, respectively), suggesting more efficient efflux of ciprofloxacin by the mutated protein (Fig. 4). Conversely, strains of both species expressing mutant AcrB accumulated more doxorubicin and minocycline, indicating reduced efflux of these compounds (Fig. 4 *A* and *C*). In addition, *Salmonella* and *E. coli* with G288D AcrB extruded doxorubicin less than strains with wild-type AcrB (Fig. 4 *B* and *D*). These data support the hypothesis that the G288D mutation in AcrB improves efflux of ciprofloxacin and so confers resistance to ciprofloxacin (and other fluoroquinolones) while perturbing doxorubicin and minocycline binding and reducing efflux, so increasing susceptibility to these agents. This discrepancy in efflux of different drug classes is explained by our computational and structural analysis of drug binding into the distal pocket, which revealed distinct and nonoverlapping modes of binding for these drug classes (Fig. 3). Other substitutions at residue 288 were also constructed by site-directed mutagenesis. These too affected susceptibility to and accumulation of ciprofloxacin, further supporting the importance of this residue in the transport function of AcrB (Fig. S6).

AcrB G288D Does Not Alter Fitness or Invasion in Vitro. Because we have previously shown that AcrB is important in the virulence of *S.* Typhimurium, we also examined whether the G288D substitution affected any other *Salmonella* attributes that could have contributed to the disseminated salmonellosis and the failure to effectively treat the patient. The G288D mutation did not alter fitness when grown in competition with a strain with wild-type AcrB (Fig. S7*A*) and did not affect invasion in the tissue culture model of infection (Fig. S7*B*).

Discussion

We have described a novel antimicrobial resistance mechanism identified by whole genome sequencing: a single nucleotide change causing MDR by alteration of the substrate specificity of an MDR efflux pump. X-ray crystallography of RND transporter proteins with substrates has proven very challenging, giving information only for three antibiotics, erythromycin, minocycline, and rifampicin (2, 5, 22). Very recently, the structure of AcrB in the presence of an efflux inhibitor has also been revealed (30). Thus, computational modeling offers a powerful and feasible alternative and has been used to predict the mechanism of efflux of numerous AcrB substrates (e.g., ref. 23). In the absence of X-ray crystallography data for AcrB cocrystallized with a fluoroquinolone antibiotic, we also used computational structural analysis of AcrB with the G288D substitution to predict any effect upon ciprofloxacin binding.

Our simulations were performed only on the apo form of the transporter. Thus, in rationalizing experimental data, we implicitly assumed that also in AcrB G288D variant the key interactions with substrates occur in the same distal binding pocket identified in the wild-type protein. Clearly, this must be proven; nonetheless, the structural modeling that we carried out demonstrated that G288D would substantially change the environment of the distal binding pocket because a bulky and charged residue would perturb the primarily hydrophobic region and in particular the conserved

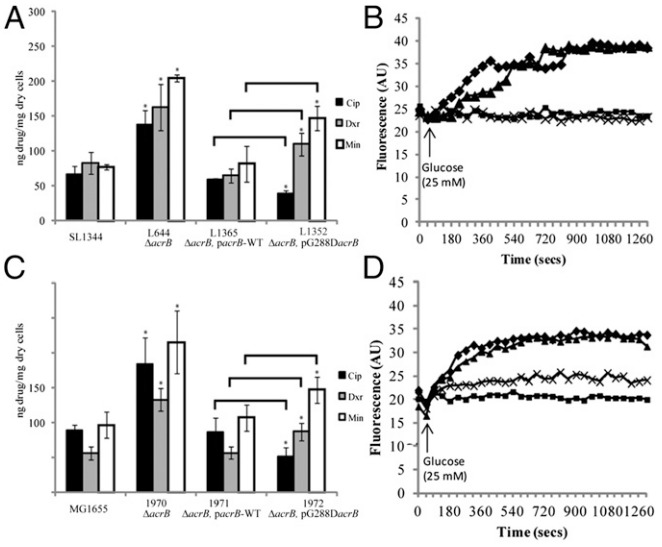

Fig. 4. The effect of the G288D mutation on the accumulation of ciprofloxacin (Cip), doxorubicin (Dxr), and minocycline (Min) and on the efflux of doxorubicin in *Salmonella* (*A* and *B*) and *E. coli* (*C* and *D*). *A* and *C* show accumulation of Cip, Dxr, and Min in *Salmonella* and *E. coli*, respectively. Black bars show Cip accumulation, gray bars show Dxr accumulation, and white bars show Min accumulation. Data presented are the mean of the steady-state values for three biological replicates ± SD. Asterisk denotes values that are significantly different from the corresponding wild-type parental strain (SL1344 or MG1655). Lines denote values, for strains carrying the G288D mutation, which are significantly different to the strain carrying the wild-type AcrB. *B* and *D* show the efflux of Dxr by *Salmonella* SL1344 and MG1655, respectively. In each case diamonds denote the wild type, squares denote Δ*acrB*, triangles denote the *acrB* mutant complemented with wild-type *acrB*, and crosses denote the *acrB* mutant complemented with G288D *acrB*.

phenylalanine cluster of the pocket. Because this site has been shown to be extremely adaptable to many substrates (27), it cannot be ruled out that despite the large effect due to G288D substitution the pocket would still be able to accommodate most compounds but with altered affinities. In agreement with such an interpretation we observed that the G288D substitution caused an increase in intracellular accumulation of doxorubicin and minocycline, which have been reported to bind to the phenylalanine cluster in the distal binding pocket (2), and concomitant increased susceptibility. In contrast, we detected decreased intracellular accumulation of, and resistance to, ciprofloxacin and other more hydrophilic drugs including tetracycline. In addition, we showed that this phenotype could be recreated in well-characterized standard strains of *Salmonella* and *E. coli*, confirming that the G288D mutation, and not any of the other SNPs detected in the clinical isolate, L18, was responsible for MDR. Thus, our modeling provided a plausible mechanistic explanation for the effect of the mutation G288D. A recent study using MD simulations has highlighted an unexpectedly complex pathway of drug expulsion, with several possible routes of export through AcrB (23). Full investigation of the interaction between drugs and the mutated protein clearly merits a systematic, stand-alone full MD simulation (e.g., ref. 27) and/or a crystallographic solution (e.g., ref. 30).

MDR in clinically relevant infections has previously been associated with overexpression of RND efflux pumps owing to mutations in regulatory genes (6). The same association was previously made for L18 (18); indeed, increased expression of *acrB* has been confirmed in this study. However, based upon our recent data showing that the bacterial cell responds to lack of efflux (irrespective of mechanism) (31), we now postulate that increased transcription of *acrB* relative to L3 is in response to altered efflux owing to the G288D substitution.

The literature contains many examples of engineered mutations in RND efflux pumps but very few naturally occurring mutations have been described, and before this study there was no indication that substitutions in AcrB would confer antibiotic resistance; the accepted dogma was that AcrB-mediated resistance was caused by overproduction of the protein. In *Salmonella* from cattle a Q733R substitution in AcrB was reported, but this had little effect on antimicrobial resistance (32). In MexD, a homolog of AcrB in *Pseudomonas aeruginosa*, SNPs in the large periplasmic loops were detected after selection on carbenicillin in the laboratory and the mutations broadened the resistance spectrum of these bacteria to include β-lactam antibiotics (33). Substitutions within AcrB have been detected following selection with various solvents but, in contrast to this study, the changes tended to be away from the drug-binding pocket and did not alter antimicrobial resistance (34–37). Mutations at codon 288 of *E. coli acrB* that were selected in vitro with the efflux pump inhibitor NMP altered susceptibility to efflux pump inhibitors and to some antimicrobial substrates (38). In contrast, in this study the G288D substitution arose during the course of clinically appropriate antimicrobial treatment and the impact was profound; the infecting organism became resistant to agents with which the patient was treated, therapy failed, and the patient died due to bacteraemia.

We have described a naturally occurring mutation in an RND efflux system that alters substrate specificity and drug susceptibility, which is a novel mechanism of antimicrobial resistance. This study also underscores the importance of whole genome sequencing in the analysis of clinically relevant antibiotic resistance and without which this new mechanism would not have been revealed. From the structural point of view, dynamics of the mutated protein must be considered to carefully account for the impact of the mutation on the functionality of the transporter. Mutation subtly affects several possible determinants responsible for the recognition and selectivity of the transporter, including orientation of side chains, polarity, electrostatic potentials, and steric properties. It is most probable that the simultaneous occurrence of these altered factors determined the different effects of the single mutation on different antibiotics. Understanding mechanisms of resistance at the genomic and structural level will not only inform clinicians treating such infections, but provide the basis for rational drug design, including new agents that are either unaffected by G288D or become more active when this substitution is present.

Materials and Methods

Strains. The clinical isolates were obtained over 5 mo (Fig. S1 and Table S3) (15). *S. enterica* serovar Typhimurium SL1344 and *E. coli* MG1655 with corresponding isogenic mutants were used for comparison (39, 40). The wild-type and G288D mutant *acrB* genes were expressed by cloning into pWKS30 as described previously (41). Further site-directed mutations at residue 288 were constructed using the Stratagene QuikChange Site Directed Mutagenesis kit.

DNA Extraction, Whole Genome Sequencing, and Data Analysis. DNA was extracted using the Invisorb Spin Cell Mini Kit according to manufacturer's instructions (Stratec). Library preparation and whole genome sequencing was carried out by Gene Pool, Edinburgh using the Illumina GAIIx platform to produce 50-bp paired-end reads. Reads were aligned against the published *S.* Typhimurium LT2 genome sequence (accession no. AE006468) using Bowtie2 (42). Read pileups were generated using Samtools mpileup, and SNPs were identified using bcftools (43). The sets of SNPs identified in L18 relative to LT2 and in L3 relative to LT2 were compared with each other using BEDtools (44) to find differences between L18 and L3. Putative mutations identified were filtered to remove those with a phred-scaled quality score of <100.

Determination of Antibiotic Resistance, Drug Accumulation, and Doxorubicin Efflux. MIC values were determined using standard methods (45). Resistance to ciprofloxacin was determined with reference to the European Committee on Antimicrobial Susceptibility Testing and Clinical and Laboratory Standards Institute recommended breakpoint concentrations. Measurement of the accumulation of ciprofloxacin and other fluoroquinolones has been previously described and is based upon the original method for norfloxacin described by Chapman and Georgopapadakou (46, 47). Doxorubicin efflux was measured directly as described previously with the following modifications (48). Cells were incubated for 1 h with 10 μM doxorubicin and 40 μM carbonyl cyanide *m*-chlorophenylhydrazone. Cells were washed and resuspended in 20 mM potassium phosphate buffer (pH 7.5) with 5 mM $MgSO_4$ and loaded into a 96-well plate. Fluorescence was measured using a Fluostar OPTIMA with excitation at 450 nm and emission at 600 nm; 25 mM glucose was injected after the first reading to energize the cells.

Measurement of *acrB* Expression with a Transcriptional *acrAB*–GFP Fusion. A GFP transcriptional reporter fusion was created with the promoter region of *acrAB* fused to GFP in the plasmid pMW82 as described previously (49). Expression of *acrAB* was measured after growth of strains to mid-logarithmic phase (OD_{600} 0.6) in MOPs minimal medium. Differences in expression were determined using *t* tests with a Bonferroni correction.

Homology Modeling and MD Simulations of *S. enterica* AcrB Wild Type and G288D Variant. To build the wild-type and the G288D AcrB structure for *S. enterica* we used the program Modeler (50) and the crystal structures of AcrB for *E. coli* (24) as reference. For each system we generated 20 different models, which were then sorted by their discrete optimized protein energy score (51). The best structures according to this criterion were selected for further MD simulations. These latter were performed using the NAMD 2.9 simulation package (52) and the ff14SB force field (53). The reduced model of AcrB (validated in ref. 27) was used for MD runs, and the protein was embedded in a 0.1 M KCl water solution [~41,000 water molecules were used, modeled with the modified TIP3P parameters (54)]. After structural optimization, the system was equilibrated by linearly increasing the temperature from 0 to 310 K in 1 ns of NPT MD simulation and equilibrated further for additional 5 ns. Then, multicopy simulations (three for each system: one of 400 ns and two of 200 ns for the wild type and three of 400 ns for the G288D system) in the NPT ensemble were performed both on the wild-type and on the G288D systems. Structural representations have been rendered using PyMol (PyMOL Molecular Graphics System; Schrödinger, LLC.) and VMD (55), and structural alignment was performed using ESPript 2.2 (56) based on a T-coffee input file (57).

Water residence times and average numbers of water molecules were calculated as previously described (58, 59) with the following alterations. First, we defined fast-, medium-, and long-time waters as those having survival probabilities τ of less than 100 ps, between 100 ps and 1 ns, and higher than 1 ns, respectively. Second, because we saved trajectory frames every 10 ps, there was no need to use a stretched exponential to fit survival probability profiles. Radii of gyration were calculated for residues lining the distal pocket (27) using the cpptraj module of Amber 14 (60).

ACKNOWLEDGMENTS. This work was funded in part by Medical Research Council Programme Grant G0501415 (to L.J.V.P.). We also acknowledge funding from ITN-2014-607694-Translocation.

1. Howell L, ed (2013) *Global Risks 2013: An initiative of the Risk Response Network* (World Economic Forum, New York).
2. Murakami S, Nakashima R, Yamashita E, Matsumoto T, Yamaguchi A (2006) Crystal structures of a multidrug transporter reveal a functionally rotating mechanism. *Nature* 443(7108):173–179.
3. Seeger MA, et al. (2006) Structural asymmetry of AcrB trimer suggests a peristaltic pump mechanism. *Science* 313(5791):1295–1298.
4. Husain F, Bikhchandani M, Nikaido H (2011) Vestibules are part of the substrate path in the multidrug efflux transporter AcrB of *Escherichia coli*. *J Bacteriol* 193(20): 5847–5849.
5. Nakashima R, Sakurai K, Yamasaki S, Nishino K, Yamaguchi A (2011) Structures of the multidrug exporter AcrB reveal a proximal multisite drug-binding pocket. *Nature* 480(7378):565–569.
6. Blair JMA, Richmond GE, Piddock LJV (2014) Multidrug efflux pumps in Gram-negative bacteria and their role in antibiotic resistance. *Future Microbiol* 9(10):1165–1177.
7. Olliver A, Vallé M, Chaslus-Dancla E, Cloeckaert A (2004) Role of an *acrR* mutation in multidrug resistance of in vitro-selected fluoroquinolone-resistant mutants of *Salmonella enterica* serovar Typhimurium. *FEMS Microbiol Lett* 238(1):267–272.
8. Webber MA, Talukder A, Piddock LJV (2005) Contribution of mutation at amino acid 45 of AcrR to *acrB* expression and ciprofloxacin resistance in clinical and veterinary *Escherichia coli* isolates. *Antimicrob Agents Chemother* 49(10):4390–4392.
9. van der Straaten T, Janssen R, Mevius DJ, van Dissel JT (2004) Salmonella gene *rma* (ramA) and multiple-drug-resistant *Salmonella enterica* serovar typhimurium. *Antimicrob Agents Chemother* 48(6):2292–2294.
10. Warner DM, Shafer WM, Jerse AE (2008) Clinically relevant mutations that cause derepression of the *Neisseria gonorrhoeae* MtrC-MtrD-MtrE Efflux pump system confer different levels of antimicrobial resistance and *in vivo* fitness. *Mol Microbiol* 70(2):462–478.
11. Kaatz GW, Thyagarajan RV, Seo SM (2005) Effect of promoter region mutations and *mgrA* overexpression on transcription of *norA*, which encodes a *Staphylococcus aureus* multidrug efflux transporter. *Antimicrob Agents Chemother* 49(1):161–169.
12. Webber MA, Piddock LJV (2001) Absence of mutations in *marRAB* or *soxRS* in *acrB*-overexpressing fluoroquinolone-resistant clinical and veterinary isolates of *Escherichia coli*. *Antimicrob Agents Chemother* 45(5):1550–1552.
13. Blair JMA, Webber MA, Baylay AJ, Ogbolu DO, Piddock LJV (2015) Molecular mechanisms of antibiotic resistance. *Nat Rev Microbiol* 13(1):42–51.
14. Piddock LJ, Griggs DJ, Hall MC, Jin YF (1993) Ciprofloxacin resistance in clinical isolates of *Salmonella typhimurium* obtained from two patients. *Antimicrob Agents Chemother* 37(4):662–666.
15. Piddock LJV, Whale K, Wise R (1990) Quinolone resistance in *salmonella*: Clinical experience. *Lancet* 335(8703):1459.
16. Ricci V, Piddock LJV (2009) Ciprofloxacin selects for multidrug resistance in *Salmonella enterica* serovar Typhimurium mediated by at least two different pathways. *J Antimicrob Chemother* 63(5):909–916.
17. Gensberg K, Jin YF, Piddock LJV (1995) A novel *gyrB* mutation in a fluoroquinolone-resistant clinical isolate of *Salmonella* typhimurium. *FEMS Microbiol Lett* 132(1-2): 57–60.
18. Piddock LJV, White DG, Gensberg K, Pumbwe L, Griggs DJ (2000) Evidence for an efflux pump mediating multiple antibiotic resistance in *Salmonella enterica* serovar Typhimurium. *Antimicrob Agents Chemother* 44(11):3118–3121.
19. Griggs DJ, Gensberg K, Piddock LJ (1996) Mutations in *gyrA* gene of quinolone-resistant *Salmonella* serotypes isolated from humans and animals. *Antimicrob Agents Chemother* 40(4):1009–1013.
20. Ruggerone P, Murakami S, Pos KM, Vargiu AV (2013) RND efflux pumps: Structural information translated into function and inhibition mechanisms. *Curr Top Med Chem* 13(24):3079–3100.
21. Hinchliffe P, Symmons MF, Hughes C, Koronakis V (2013) Structure and operation of bacterial tripartite pumps. *Annu Rev Microbiol* 67(1):221–242.
22. Eicher T, et al. (2012) Transport of drugs by the multidrug transporter AcrB involves an access and a deep binding pocket that are separated by a switch-loop. *Proc Natl Acad Sci USA* 109(15):5687–5692.
23. Yao X-Q, Kimura N, Murakami S, Takada S (2013) Drug uptake pathways of multidrug transporter AcrB studied by molecular simulations and site-directed mutagenesis experiments. *J Am Chem Soc* 135(20):7474–7485.
24. Sennhauser G, Amstutz P, Briand C, Storchenegger O, Grütter MG (2007) Drug export pathway of multidrug exporter AcrB revealed by DARPin inhibitors. *PLoS Biol* 5(1):e7.
25. Vargiu AV, et al. (2011) Effect of the F610A mutation on substrate extrusion in the AcrB transporter: Explanation and rationale by molecular dynamics simulations. *J Am Chem Soc* 133(28):10704–10707.
26. Bohnert JA, et al. (2008) Site-directed mutagenesis reveals putative substrate binding residues in the *Escherichia coli* RND efflux pump AcrB. *J Bacteriol* 190(24):8225–8229.
27. Vargiu AV, Nikaido H (2012) Multidrug binding properties of the AcrB efflux pump characterized by molecular dynamics simulations. *Proc Natl Acad Sci USA* 109(50): 20637–20642.
28. Kinana AD, Vargiu AV, Nikaido H (2013) Some ligands enhance the efflux of other ligands by the *Escherichia coli* multidrug pump AcrB. *Biochemistry* 52(46):8342–8351.
29. Vargiu AV, Ruggerone P, Opperman TJ, Nguyen ST, Nikaido H (2014) Inhibition of *E. coli* AcrB multidrug efflux pump by MBX2319: Molecular mechanism and comparison with other inhibitors. *Antimicrob Agents Ch* 58(10):6224–6234.
30. Nakashima R, et al. (2013) Structural basis for the inhibition of bacterial multidrug exporters. *Nature* 500(7460):102–106.
31. Lawler AJ, Ricci V, Busby SJW, Piddock LJV (2013) Genetic inactivation of *acrAB* or inhibition of efflux induces expression of *ramA*. *J Antimicrob Chemother* 68(7): 1551–1557.
32. Elkins CA, Mullis LB, Lacher DW, Jung CM (2010) Single nucleotide polymorphism analysis of the major tripartite multidrug efflux pump of *Escherichia coli*: Functional conservation in disparate animal reservoirs despite exposure to antimicrobial chemotherapy. *Antimicrob Agents Chemother* 54(3):1007–1015.
33. Mao W, et al. (2002) On the mechanism of substrate specificity by resistance nodulation division (RND)-type multidrug resistance pumps: The large periplasmic loops of MexD from *Pseudomonas aeruginosa* are involved in substrate recognition. *Mol Microbiol* 46(3):889–901.
34. Foo JL, Leong SSJ (2013) Directed evolution of an *E. coli* inner membrane transporter for improved efflux of biofuel molecules. *Biotechnol Biofuels* 6(1):81.
35. Fisher MA, et al. (2014) Enhancing tolerance to short-chain alcohols by engineering the *Escherichia coli* AcrB efflux pump to secrete the non-native substrate n-butanol. *ACS Synth Biol* 3(1):30–40.
36. Minty JJ, et al. (2011) Evolution combined with genomic study elucidates genetic bases of isobutanol tolerance in *Escherichia coli*. *Microb Cell Fact* 10:18.
37. Mingardon F, et al. (2014) Improving olefin tolerance and production in *E. coli* using native and evolved AcrB. *Biotechnol Bioeng*, 10.1002/bit.25511.
38. Schuster S, et al. (2014) Random mutagenesis of the multidrug transporter AcrB from Escherichia coli for identification of putative target residues of efflux pump inhibitors. *Antimicrob Agents Chemother* 58(11):6870–6878.
39. Wray C, Sojka WJ (1978) Experimental *Salmonella typhimurium* infection in calves. *Res Vet Sci* 25(2):139–143.
40. Eaves DJ, Ricci V, Piddock LJV (2004) Expression of *acrB, acrF, acrD, marA*, and *soxS* in *Salmonella enterica* serovar Typhimurium: Role in multiple antibiotic resistance. *Antimicrob Agents Chemother* 48(4):1145–1150.
41. Buckley AM, et al. (2006) The AcrAB-TolC efflux system of *Salmonella enterica* serovar Typhimurium plays a role in pathogenesis. *Cell Microbiol* 8(5):847–856.
42. Langmead B, Salzberg SL (2012) Fast gapped-read alignment with Bowtie 2. *Nat Methods* 9(4):357–359.
43. Li H, et al.; 1000 Genome Project Data Processing Subgroup (2009) The Sequence Alignment/Map format and SAMtools. *Bioinformatics* 25(16):2078–2079.
44. Quinlan AR, Hall IM (2010) BEDTools: A flexible suite of utilities for comparing genomic features. *Bioinformatics* 26(6):841–842.
45. Andrews JM; BASC Working Party on Susceptibility Testing (2006) BSAC standardized disc susceptibility testing method (version 5). *J Antimicrob Chemother* 58(3):511–529.
46. Chapman JS, Georgopapadakou NH (1988) Routes of quinolone permeation in *Escherichia coli*. *Antimicrob Agents Chemother* 32(4):438–442.
47. Mortimer PGS, Piddock LJV (1991) A comparison of methods used for measuring the accumulation of quinolones by *Enterobacteriaceae, Pseudomonas aeruginosa* and *Staphylococcus aureus*. *J Antimicrob Chemother* 28(5):639–653.
48. Nishino K, Yamaguchi A (2001) Overexpression of the response regulator *evgA* of the two-component signal transduction system modulates multidrug resistance conferred by multidrug resistance transporters. *J Bacteriol* 183(4):1455–1458.
49. Bumann D, Valdivia RH (2007) Identification of host-induced pathogen genes by differential fluorescence induction reporter systems. *Nat Protoc* 2(4):770–777.
50. Šali A, Blundell TL (1993) Comparative protein modelling by satisfaction of spatial restraints. *J Mol Biol* 234(3):779–815.
51. Shen MY, Sali A (2006) Statistical potential for assessment and prediction of protein structures. *Protein Sci* 15(11):2507–2524.
52. Phillips JC, et al. (2005) Scalable molecular dynamics with NAMD. *J Comput Chem* 26(16):1781–1802.
53. Hornak V, et al. (2006) Comparison of multiple Amber force fields and development of improved protein backbone parameters. *Proteins* 65(3):712–725.
54. Jorgensen WL, Chandrasekhar J, Madura JD, Impey RW, Klein ML (1983) Comparison of simple potential functions for simulating liquid water. *J Chem Phys* 79(2):926–935.
55. Humphrey W, Dalke A, Schulten K (1996) VMD: Visual molecular dynamics. *J Mol Graph* 14(1):33–38, 27–28.
56. Gouet P, Courcelle E, Stuart DI, Métoz F (1999) ESPript: Analysis of multiple sequence alignments in PostScript. *Bioinformatics* 15(4):305–308.
57. Notredame C, Higgins DG, Heringa J (2000) T-Coffee: A novel method for fast and accurate multiple sequence alignment. *J Mol Biol* 302(1):205–217.
58. Sterpone F, Ceccarelli M, Marchi M (2001) Dynamics of hydration in hen egg white lysozyme. *J Mol Biol* 311(2):409–419.
59. Collu F, Ceccarelli M, Ruggerone P (2012) Exploring binding properties of agonists interacting with a δ-opioid receptor. *PLoS ONE* 7(12):e52633.
60. Case DA, et al. (2014) *Amber 14* (Univ of California, San Francisco).